CLAS-NOTE 2003-005
March 14, 2003

Momentum Corrections for E6

Alexei Klimenko and Sebastian Kuhn
Old Dominion University

1 Introduction

In this note, we describe a new method to correct particle momenta as measured by CLAS and reconstructed with RECSIS for electron runs. This method was used to correct all measured particle momenta (electrons and hadrons) for the Physics analysis of E6. However, it was also tested for EG1b analysis and should be applicable in general for all CLAS analyses (maybe with some modifications). Our goal was to develop a *general, consistent* and *realistic* scheme which should allow us to simultaneously correct momenta and polar angles of *all* final state particles.

It is well known that the particle momenta as reconstructed by RECSIS (or A1c) show systematic deviations, as evidenced by shifted and broadened W distributions for inclusive data and missing mass peaks for more exclusive data. In inclusive data, the centroid for the W distribution of the elastic peak is moved from is theoretical value, $W = M_p = 0.9382$ GeV and significantly broader than expected from the intrinsic momentum resolution of CLAS. A clear dependence of the shift on both ϕ_e and, to a lesser extent, θ_e is observed (see Figs. 1 and 2). These systematic momentum deviations could in principle arise from several sources:

- Misalignment of the drift chambers relative to their nominal positions, inaccurate or out–of–date survey results
- Neglect to properly incorporate effects like wire sag, wire take-off position on the "trumpet lips", thermal and stress distortions of the drift chambers, and other factors affecting wire position

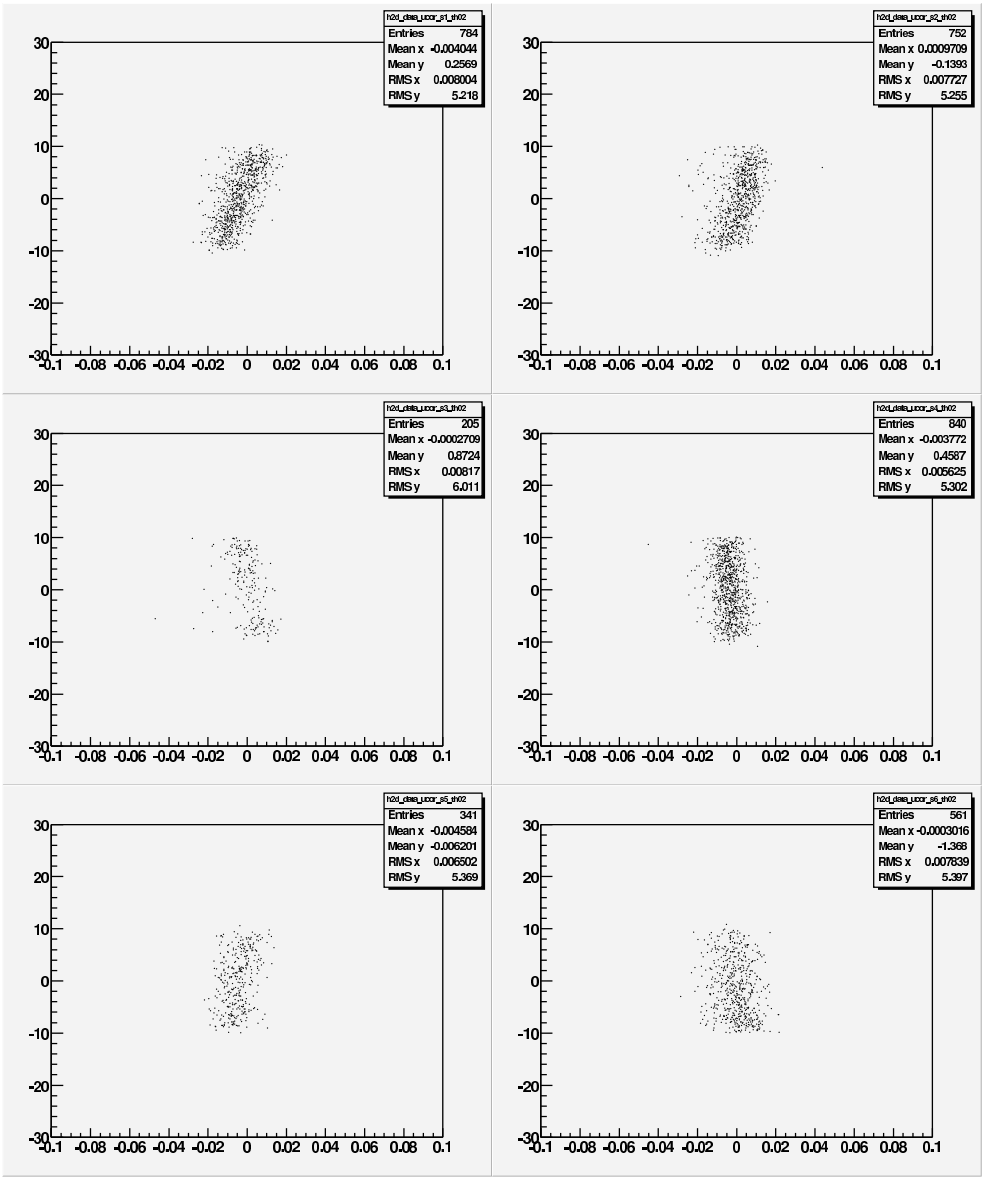

Figure 1: Relative difference $\Delta p/p$ between reconstructed electron momentum and calculated momentum for elastic scattering off a proton (see Eq. 1) plotted (on the x-axis) versus the azimuthal angle ϕ in the sector system (on the y-axis) for all 6 sectors of CLAS. The data are for electron scattering angle $\theta_e = 18^\circ$ and inbending torus polarity. A clear correlation of the momentum deviation with ϕ is visible in nearly all sectors.

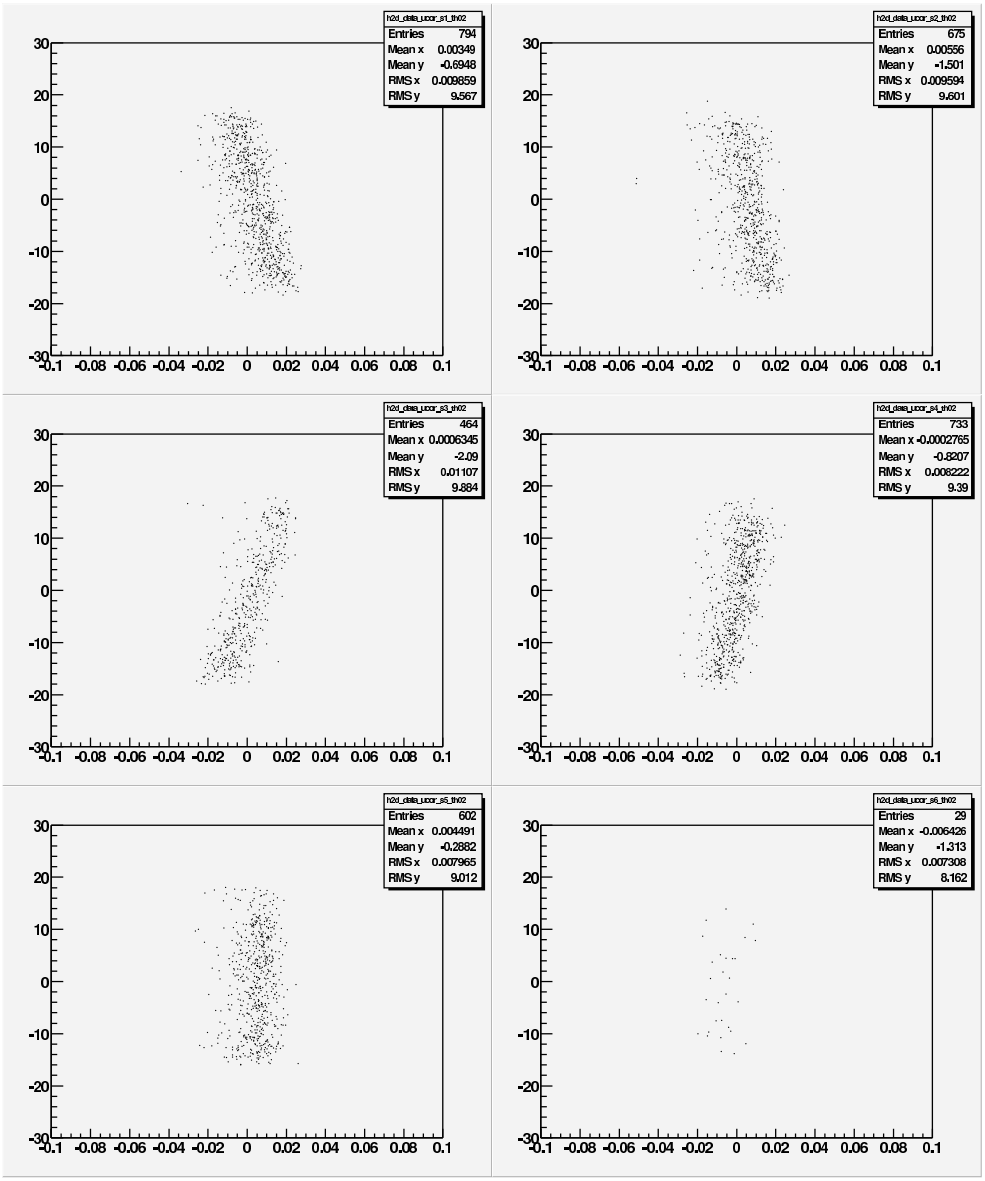

Figure 2: Same as Fig. 1 but for data taken with *outbending* torus polarity. The correlation of the momentum deviation with ϕ has the opposite sign to that in Fig. 1, indicating a dependence on the sign of the magnetic field.

- Insufficient or incorrect information in the reconstruction code on the exact location of the wire feedthrough holes in the drift chamber endplates as actually drilled, especially for the very complicated compound angles involved in the stereo superlayers
- Incomplete knowledge of the torus (or mini–torus) magnetic field distribution

The first three of these possible error sources could affect both the reconstructed angle and the momentum, while the last item affects the momentum only.

In the past, there have been several schemes tried and employed to at least approximately correct for these errors. One widely used method first proposed by Volker Burkert (used, for instance, for EG1a, see also CLAS Note 2001-008) assumed that the angles are basically reconstructed correctly and corrects the electron momenta for inclusive elastic events to agree with their theoretical value,

$$E'_{\rm elastic} = \frac{E_{beam}}{1 + \frac{2E_{beam}}{M_p}\sin^2(\theta_e/2)} \tag{1}$$

Under the assumption that the momentum deviation is due to a somewhat incorrect map of the CLAS torus magnetic field, the correction is applied by multiplying the measured electron momenta with a factor which is typically parametrized as a function of θ_e and ϕ_e. A drawback of this method is that the correction function is somewhat ad–hoc and has to be extrapolated into the inelastic region (corresponding to lower electron momenta) where it is not constrained by data. There is also no obvious way to extend the correction to other particles or other running conditions (torus currents). Finally, the assumption that angles are reconstructed correctly may be unjustified (see, e.g., CLAS Note 2002-008).

Other attempts have been made to address some of the possible misalignment problems using straight track data and to improve the momentum resolution by varying the magnetic field map for the torus magnet (there exist now two different field maps, termed "old" and "new", and most run groups

use some mix of those two to optimize their resolution, e.g. 34% "old" and 66% "new"). There have also been several more sophisticated attempts to correct both angles and momenta, both for electrons and other particles (see, e.g., K.-J. Park's web site at http://www.jlab.org/∼parkkj/index_pre.html and CLAS Note 2001-18). Most methods that we are aware of concentrate (or at least start) with elastically scattered electrons and then make assumptions about at least two parameters (e.g., the beam energy and the proton scattering angle are "known absolutely") to determine very detailed corrections for electron momenta and/or angles. Again, the results can not necessarily be extended into the inelastic region and to other particles (which may receive different ad–hoc corrections to improve missing mass distributions).

Our approach has been to make some basic assumptions about the **form** of the necessary corrections, with a modest amount of free parameters (14 per sector), and then attempt a simultaneous fit over a large, heterogeneous data set (including elastic and inelastic events and several different particle types and torus settings) to fix these parameters. The result is a uniform correction algorithm for all momenta and all polar angles which should improve all missing mass and W spectra. Our method is most similar to the one explained in CLAS Note 2001-18, which is based on similar assumptions. However, our method includes corrections to the polar angles as well as the momenta and uses multi–particle final states in addition to elastic events.

2 Theoretical background

We assume that both momenta and polar angles are distorted by systematic displacements of the drift chambers and by magnetic field deviations from the field map used in the reconstruction code. In the following, we first discuss the effects of drift chamber displacements on angle and momenta and then add a correction due to field variations.

We found that the most pronounced improvement in reconstructed momenta (including resolution in W) can be achieved by parametrizing the drift chamber dislocations with 8 fit parameters in each sector, which roughly correlate to a displacement in z (along the beam) and x (away from the beam axis) as well as a "yaw" (phi-depend z-displacement) and a "roll" (phi-

dependent x-displacement) for each Region 2 and Region 3 chamber. (We have to keep *something* fixed in this scheme, so we decided to leave Region 1 unchanged.) We do *not* correct the azimuthal (ϕ) angles, since they are determined with larger intrinsic uncertainty and seem to have fewer problems (e.g., the difference $\phi_e - \phi_p$ for elastic events usually is centered on the correct value of 180 degrees). They also affect reconstructed kinematical quantities less in the case of E6.

The effect of these displacements on a given reconstructed track can be written as a change $\Delta\theta$ in the polar scattering angle and Δp in the momentum:

$$\Delta\theta = (A + B\phi)\frac{\cos\theta}{\cos\phi} + (C + D\phi)\sin\theta \tag{2}$$

and

$$\frac{\Delta p}{p} = \left((E + F\phi)\frac{\cos\theta}{\cos\phi} + (G + H\phi)\sin\theta\right)\frac{p}{qB_{\rm Torus}}. \tag{3}$$

Here, q is the particle charge in units of e, p the RECSIS reconstructed momentum in GeV, and θ and $\phi = \phi_e - \phi_{\rm Sector}$ are the RECSIS reconstructed polar and azimuthal angle (the latter measured in the **sector** relative coordinate system where $\phi = 0$ in the sector midplane). The quantity $B_{\rm Torus}$ really stands for the integral $\int B_{\rm trans} d\ell$ along the path of the track, converted to GV by multiplying with $c = 0.29979$ m/ns. The ratio $qB_{\rm Torus}/p$ is proportional to the amount of curvature of the track, which determines the effect of a misalignment of the drift chambers. Using the CLAS CDR, we found a simple parametrization of this integral as function of θ:

$$B_{Torus} = 0.76\frac{I_{Torus}\sin^2 4\theta}{3375\ \theta/\mathrm{rad}} \text{ for } \theta < \pi/8 \text{ and } B_{Torus} = 0.76\frac{I_{Torus}}{3375\ \theta/\mathrm{rad}} \text{ for } \theta \geq \pi/8 \tag{4}$$

which is good enough for this purpose - the overall normalization is unimportant since it will be absorbed in the definition of the parameters $E - H$.

Parameters A and E describe displacements of Region II and/or Region III drift chambers radially outward which affect mostly forward–going

particles (hence the factor $cos(\theta)$), while B and F can be interpreted as ϕ–dependent radial displacements (a "roll" or rotation around the beam axis). Similarly, C and G describe displacements along the beam axis (affecting mostly particles at large scattering angles) and D and F correspond to a "yaw" (a rotation around the radial direction). We found little improvement in our fits (and considerably less constrained parameters) if we also included a rotation around the wire direction (a "pitch"), therefore, we didn't include parameters for this degree of freedom (nor for displacements in the direction of the wires). While there is a one–to–one correspondence between the eight parameters listed here and the assumed displacements and rotations of both Region II and Region III drift chambers, the relationship is complicated and not really essential as long as the parametrization of Eqs. 2 – 4 gives a good overall fit.

In addition to the angle and momentum corrections due to drift chamber displacements described above, there could be an additional shift in the reconstructed momenta from differences between the magnetic field map encoded in the reconstruction software and the actual spatial distribution of the CLAS torus magnetic field. This contribution is typically considered to be the main (or only) effect in the "standard" electron momentum correction method pioneered by V. Burkert. It can be incorporated by adding another function $f(\theta, \phi)$ to Eq. 3 which should depend only weakly (if at all) on the momentum itself. Through many trials and errors, we arrived at the following parametrization:

$$f = (J\cos(\theta) + K\sin(\theta) + L\sin(2\theta)) + (M\cos(\theta) + N\sin(\theta) + O\sin(2\theta))\,\phi \tag{5}$$

with another 6 parameters $J - O$. In principle, other functional forms could be tried and might work better for other run groups. However, it is very important to chose a function that is "well–behaved" over the full range of angles θ, in our case from 10 degrees to 140 degrees, since our goal is to apply the corrections equally to *all* particle tracks.

It is very important to note that the two parts of the momentum correction behave completely differently under reversal of charge or magnetic field sign and have different dependence on particle momentum. The correction for magnetic field uncertainties leads to a uniform correction factor $f(\theta, \phi)$ which should (in principle) be applied to *all* momenta (independent of particle charge and momentum or torus field strength and sign). In contrast,

the correction due to drift chamber position uncertainties leads to a correction that changes sign with particle charge and torus field and is directly proportional to particle momentum and inversely proportional to torus field strength. Of course, if one uses only elastically scattered electrons and a single torus field setting to determine the correction, one cannot distinguish between these two contributions, since there is a complete correlation between electron momentum and angle and therefore any momentum–dependence of the correction can be absorbed into the θ–dependence of the function $f(\theta, \phi)$ (Eq. 5). However, by comparing the momentum deviations for opposite torus fields (Figs. 1 and 2) one can see that there is a sizable part of the correction that reverses sign with the torus field, in agreement with the form of the correction in Eq. 3. It is therefore important to use data samples containing both positively and negatively charged particles, with a wide range in momenta at any given scattering angle, covering a large part of the physical acceptance of CLAS. It is also very beneficial to include data with both positive and negative torus current in the fit, since this will very effectively decouple the two parts of the momentum correction. While it is possible to get as good (or even better) improvements in the resolution of the elastic peak by using only corrections of the form Eq. 5, these corrections would have the wrong behavior if extrapolated to lower momenta (inelastically scattered electrons), positively charged particles and different torus fields.

Once the 14 parameters $A - O$ have been determined for each sector, we can correct the RECSIS reconstructed angle θ by adding $\Delta\theta$ and the RECSIS reconstructed momentum p by multiplying it with $(1 + \frac{\Delta p}{p})$. We determine these parameters by first selecting samples of fully reconstructed (exclusive) events where all final state particles are detected, and then applying four-momentum conservation to each of them to extract a "goodness of fit" variable like χ^2 which we then optimize for all these events. The most obvious candidate for such events are elastic $p(e, e'p)$with both proton and electron detected. However, it is also important to use more complicated events, with low momentum particles (protons and pions) covering a range of angles. One could use fully reconstructed $p(e, e'p\pi^+\pi^-)$ events. For E6, we included $d(e, epp\pi^-)$ events since they most closely resemble the events of interest for our analysis and since we have data on both proton and deuteron targets. The goodness of fit is basically the squared difference between each of the 4 components of the initial state four-vector $(E, 0, 0, E) + (M, 0, 0, 0)$ and the final state four-vector, e.g. $(E', \mathbf{p'_{el}}) + (E_p, \mathbf{p_{proton}})$. We add the four

squares together, each weighted by a reasonable estimate of the "intrinsic" resolution CLAS should have for them. (We assume 20 MeV resolution for the energy and the z-component and 14 MeV resolution for the transverse components of the momentum.)

3 Preliminaries

For *any* momentum correction scheme, it is important not to make things worse by introducing an unwanted bias into the fit. Possible problems can arise from several areas, but especially from incorrect beam energy, failure to account for ionization (and possibly radiative) energy losses, and bias in event sample selection. We discuss these "preliminaries" in a little bit more detail below.

The actual energy of the electrons in the beam (or, more precisely, in the center of the target) enters directly in the values of computed kinematic variables like W, Q^2 and missing mass. For our momentum correction fit, it also enters since one of the four 4-momentum conservation equations contains the beam energy. If a wrong beam energy is assumed, one can easily bias the fit which tries to "recenter" the kinematic variables at their proper values. Unfortunately, most CLAS data are (at least initially) analyzed with the default value of the beam energy which is stored in the database. As best as we can tell, this value corresponds to the "set energy" of the accelerator, which in the past has been shown to deviate by as much as 10-20 MeV from the "true" beam energy, especially at high energies above 5 GeV (see CLAS Note 2002-008). One possible remedy is to check for beam energy measurements done in one of the other Halls (especially Hall A) during the time of the CLAS experiment (see, e.g., the table found at http://hallaweb.jlab.org/equipment/beam/brittin/beam_energy_table.html) and scale these energies using the Equation $E_B = E_A(n_B{+}0.056)/(n_A{+}0.056)$ where n_A and n_B are the number of passes for the two halls. Another method is using elastic $p(e,e'p)$ events directly to calculate the beam energy from the measured proton and electron angles (without any need for measured momenta) – see CLAS Note 2002-008. This method requires to first use tight cuts to select truly elastic events (see below in the Section on "Event Selec-

tion"). For each event passing these cuts, fill a histogram of

$$E_{\rm beam} = M_p \left(\frac{1}{\tan(\theta_e/2)\tan(\theta_p)} - 1 \right). \qquad (6)$$

In the case of composite targets (for instance NH_3 in EG1 or CH_2 in E2) it also helps to subtract the background from nitrogen or carbon from the histogram. Then fit a Gaussian to the peak (restricting the fit range to roughly 2 standard deviations in each direction) and extract the mean as best estimate for the "true" beam energy. Ideally, one should run a first iteration of our correction algorithm to correct the scattering angles θ_e and θ_p before using them in this manner.

A second systematic bias comes from energy loss of outgoing particles due to both ionization and radiation. While radiation losses affect mostly electrons, ionization losses are important for low–momentum hadrons which are supposed to be included in the fit to make it applicable to all kinematic regions (e.g., from the reaction $p(e, e'p\pi^+\pi^-)$). We found that one can ignore radiative losses of the electron provided one uses a fairly narrow cut on the missing energy of the events selected for the fit (see next Section). We chose a missing energy cut of ± 60 MeV. On the other hand, since RECSIS doesn't include energy loss effects in its reconstructed track parameters, one has to **add** the most likely energy lost by a given particle to its reconstructed (and corrected) energy before checking 4-momentum conservation at the vertex. One can either use GSIM for these corrections, or (in our case) develop a simple approximation of the energy loss as a function of scattering angle, particle mass and momentum, based on fits to energy loss curves (see, e.g., the TRIUMF kinematic handbook). Our fit takes the form

$$E_{\rm kin}({\rm vertex}) = \left[E^b_{\rm kin}({\rm track}) + \frac{m_{\rm particle}}{M_p} \left(a_1 + \frac{a_2}{\sin(\theta)} \right) \right]^{1/b}. \qquad (7)$$

Here, $E_{\rm kin} = \sqrt{m^2 + p^2} - m$ is the kinetic energy of the particle. The exponent b and the parameters a_1 and a_2 are determined by a fit to several low–momentum proton tracks. This correction is applied in the following sequence: First, the track momentum as reconstructed by RECSIS is corrected by our algorithm. Then, it is converted to kinetic energy $E_{\rm kin}({\rm track})$ and the kinetic energy at the vertex is calculated using Eq. 7. Finally, this kinetic energy is converted back to the momentum at the vertex and the relative

increase $p(\text{vertex})/p(\text{track}) - 1$ is calculated. Once this relative increase in the momentum has been determined, all momentum components have to be scaled accordingly.

Finally, if the initial momenta are far away from their proper values (as we found in the case of outbending electrons for E6), there may be an inherent bias in the event selection (see below). Since we require a missing energy of less than 60 MeV, a shift by about 20 MeV in reconstructed momenta could yield a skewed distribution of "true" initial momenta, with roughly twice more on one side of the peak than on the other. The best apparent solution is to do the fit iteratively, by first determining a preliminary set of corrections, then using these to select a "better" sample of events within cuts.

The remainder of this note describes how the optimum sets of parameters $A - O$ are determined for each sector. Once these parameters and the "true" beam energy (see above) are given (6 times 14 = 84 parameters total), one can simple apply Eqns. 2 – 5 to correct all reconstructed 4-momenta of all particles in an event. If one is only interested in inclusive electrons, no further corrections are needed. However, when studying multi-particle final states, the energy loss correction should be applied as well (*after* the momentum correction), at least for relatively slow hadrons.

4 Event selection

Our method relies on 4-momentum conservation which requires that *all* particles in the final state are detected. Furthermore, if at all possible, one should only use proton and (possibly) deuteron target runs, since nuclear targets yield uncertainties coming from Fermi momentum and binding.

We use fully reconstructed elastic events $p(e, e'p)$ as our primary sample. In addition, it is also important to use multi-particle final states if possible, to cover lower hadron momenta and avoid the strong kinematic correlation between angle and momentum for elastic events. We chose the reaction $d(e, e'pp\pi^-)$ for this purpose. Experiments that do not have a deuteron target might use exclusive $p(e, e'p\pi^-\pi^+)$ events instead.

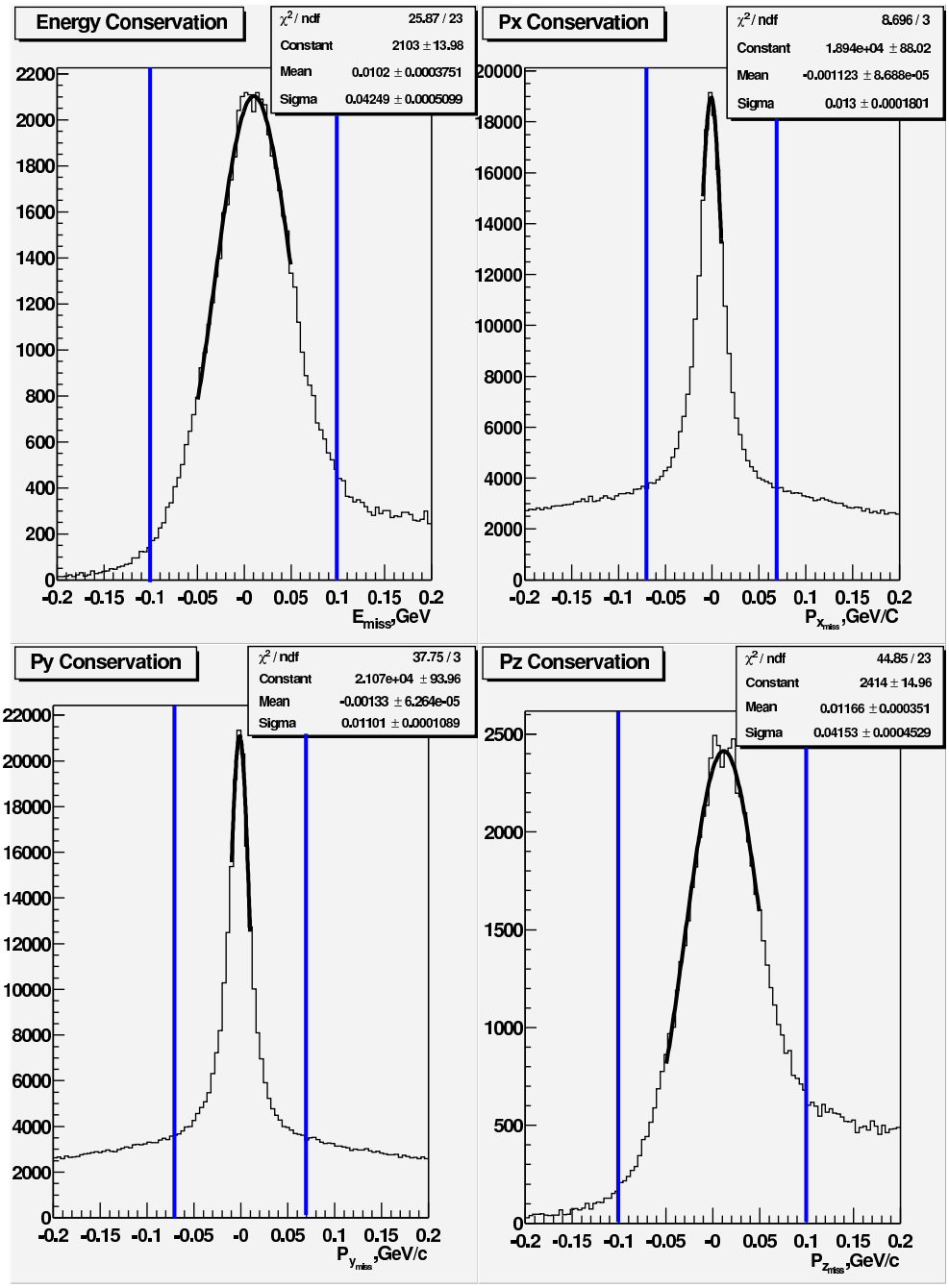

Figure 3: Example for the distribution of missing 4-momenta of uncorrected elastic events from RECSIS. The cuts applied to select the events for our fit are indicated.

Secondly, it is also very advantageous to have available runs with both positive (electron inbending) and negative (electron outbending) torus polarities. This allows a clean separation of the parameters in Eq. 3 (which depends on the torus sign) and in Eq. 4 (which does not). In a "pinch", it is probably sufficient to have *either* outbending runs *or* multi-particle final states in the event sample used for the fit. For the case of EG1b, we actually used only elastic events on NH_3 to minimize the complications from the nuclear background, but included inbending and outbending torus polarities.

For all events, we first apply the usual fiducial, vertex and electron ID cuts. We use SEB particle ID to select protons and pions. We then apply cuts on missing 4-momentum to exclude events where not all produced particles were detected in CLAS. These cuts also serve to suppress nuclear background (from target windows or, in the case of EG1, non-hydrogen target components). We calculate the missing 4-momentum of each event and then retain only events where $|E(\mathrm{miss})| \leq 0.06$ GeV, $|p_z(\mathrm{miss})| \leq 0.06$ GeV, $|p_x(\mathrm{miss})| \leq 0.05$ GeV, and $|p_y(\mathrm{miss})| \leq 0.05$ GeV, where z is the direction along the beam and x and y perpendicular to the beam. The cut on $E(\mathrm{miss})$ also serves to remove events where the electron lost a large amount of energy due to internal or external radiation (these events would otherwise skew the momentum corrections). For elastic events, we also included a cut on the difference between the angle ϕ_e of the electron and the angle ϕ_p of the proton, requiring this difference to be 180° within $\pm 1^\circ$. Figure 3 shows an example for the distribution of 4-momenta for uncorrected elastic events (E6, 5.76 GeV beam, inbending torus polarity). All momenta have been corrected for energy loss (see previous Section).

As can be seen in Fig. 3, the initial momentum distributions are fairly wide and not centered on zero. For this reason, we iterated our fit procedure once, reselecting events within our cuts after applying the first round momentum corrections for the second round fit. This led to appreciably better fits for the final results. We show the 4-momentum distributions after the first iteration in Fig. 4.

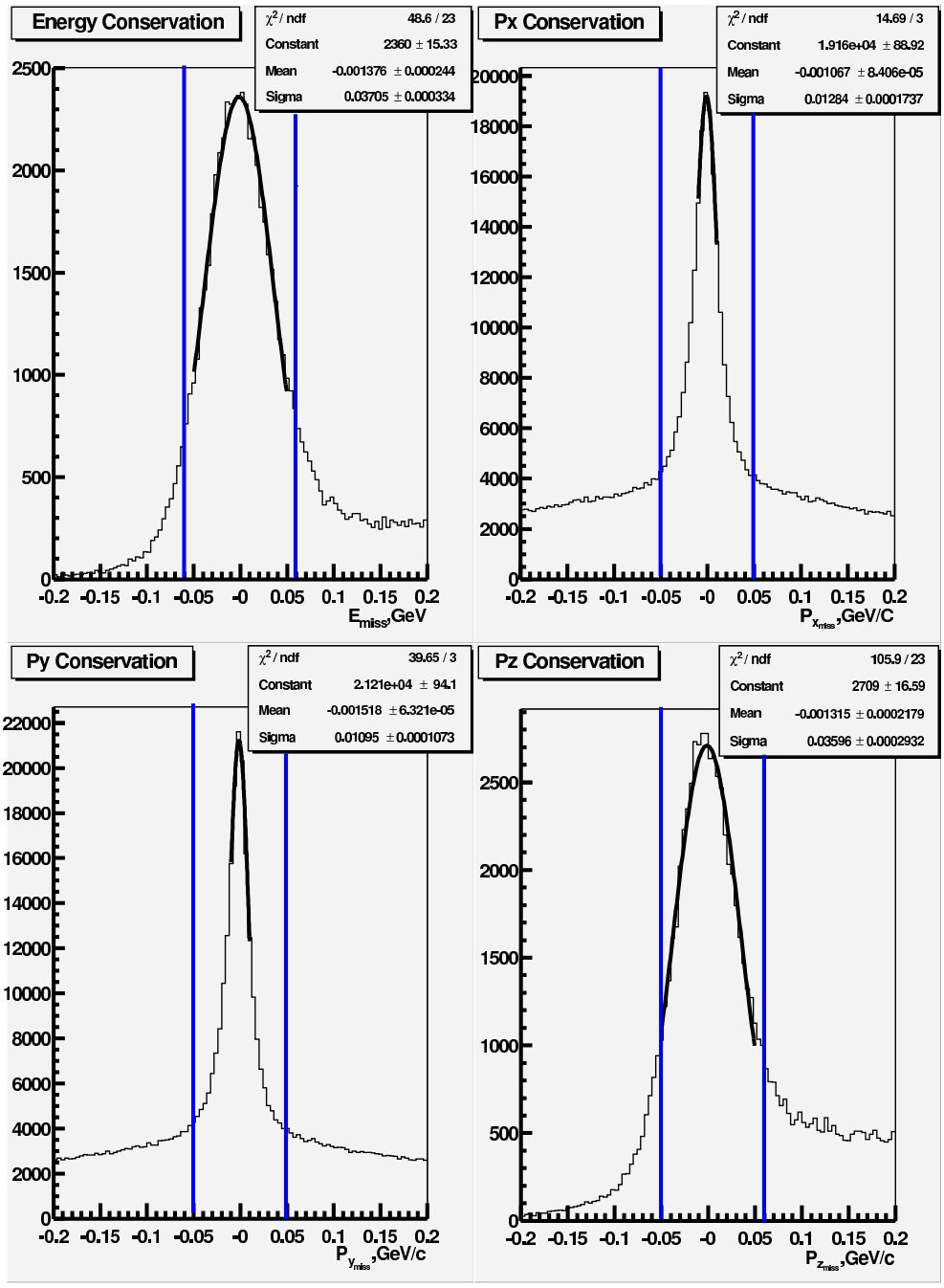

Figure 4: The distribution of missing 4-momenta of elastic events from REC-SIS after the first iteration of our fit. The cuts applied to select the events for our fit are indicated.

5 Fit procedure and results

The code for reading in events and calculating all needed quantities is written in C++ and based on ROOT. We use "MINUIT" to optimize all 84 parameters for our momentum and angle corrections. For each "trial" set of parameters, we loop over all selected exclusive events (see previous Section). For each event, we first apply the momentum corrections due to the present parameter set, then add in the energy lost due to ionization for all hadrons. We calculate all four components of the missing 4-momentum. We add the squares of these components, normalized to a "reasonable" expected resolution, to the overall χ^2 for the fit:

$$\Delta\chi^2 = \frac{E^2(\text{miss}) + p_z^2(\text{miss})}{(0.020\ \text{GeV})^2} + \frac{p_x^2(\text{miss}) + p_y^2(\text{miss})}{(0.014\ \text{GeV})^2}. \tag{8}$$

After looping over all events (inbending, outbending, elastic, multi–particle), we add 84 more terms to the total χ^2, one for each of the 84 parameters:

$$\Delta\chi^2 = \sum \frac{\text{parm}^2}{\sigma^2(\text{parm})}. \tag{9}$$

This "trick" is used to limit the parameters to "reasonable ranges" and avoid run–away solutions in some corner of parameter space. We chose a "reasonable range" for most parameters of $\sigma(\text{parm}) = 0.001$. However, due to the large ϕ–dependent correction necessary for the momentum (see Fig. 1), we increased this range to $\sigma(\text{parm}) = 0.01$ for parameters F and H for each sector (see Eq. 3).

Our final results for E6 yielded a χ^2 of 6.2 per event (1.54 per degree of freedom given the 4 components of the missing 4-momentum for each event). This can be interpreted as a slightly (25%) larger resolution in the four missing momentum components than assumed in Eq. 8. This final χ^2 is less than half of the initial one (before our first iteration).

Figures 5 – 6 show the comparison of initial and final resolution in W for inclusive electrons, and the size of the angle and momentum corrections versus scattering angle for electrons and protons, both for inbending (Fig. 5) as well as outbending (Fig. 6) torus polarity. The corrections are typically

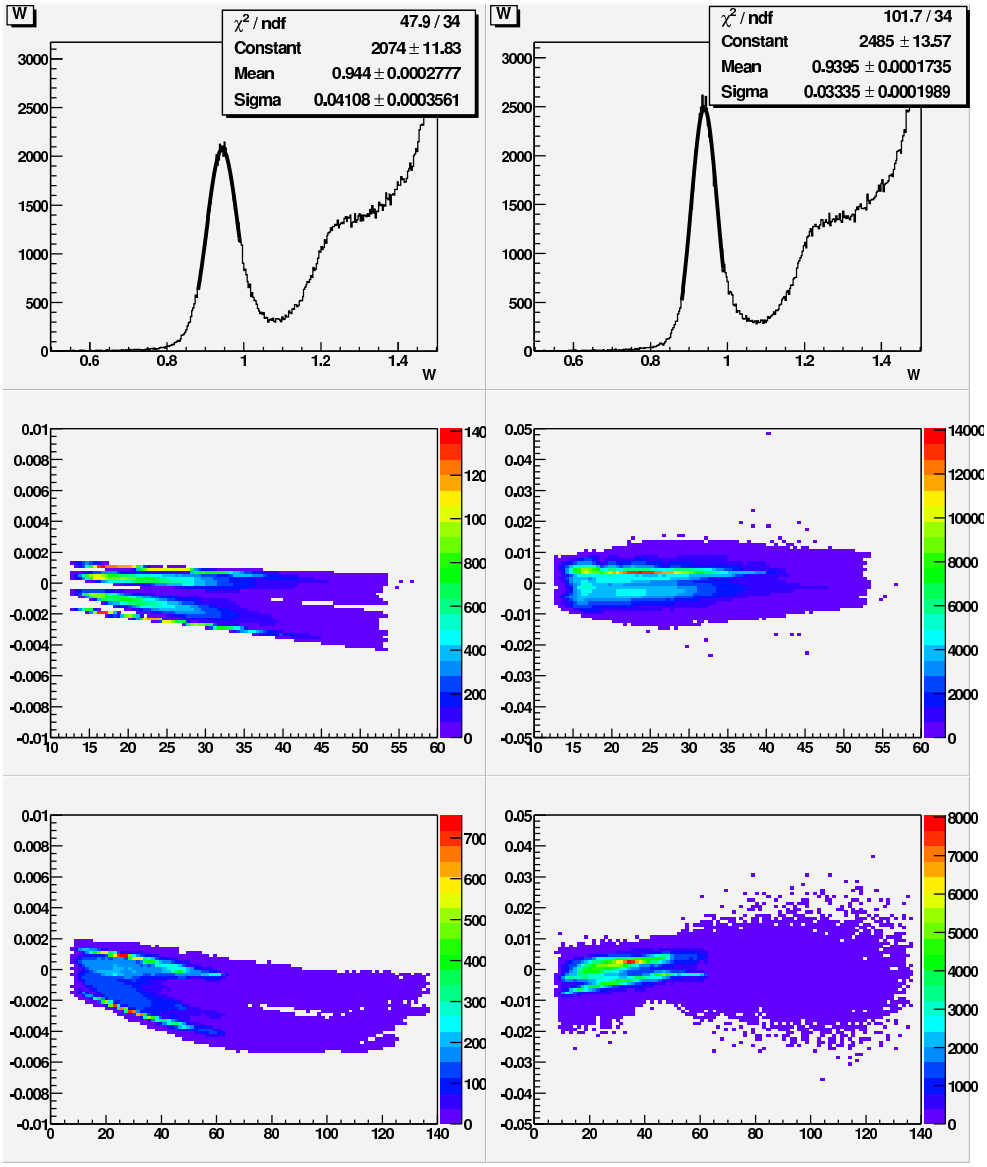

Figure 5: W distribution for inclusive electron events and inbending torus, both before (left top panel) and after (right top panel) momentum corrections. The corrections applied to polar angles (in mrad, left side) and momenta ($\Delta p/p$, right side) for all electrons (middle row) and protons (bottom row) in our data sample are shown versus scattering angle.

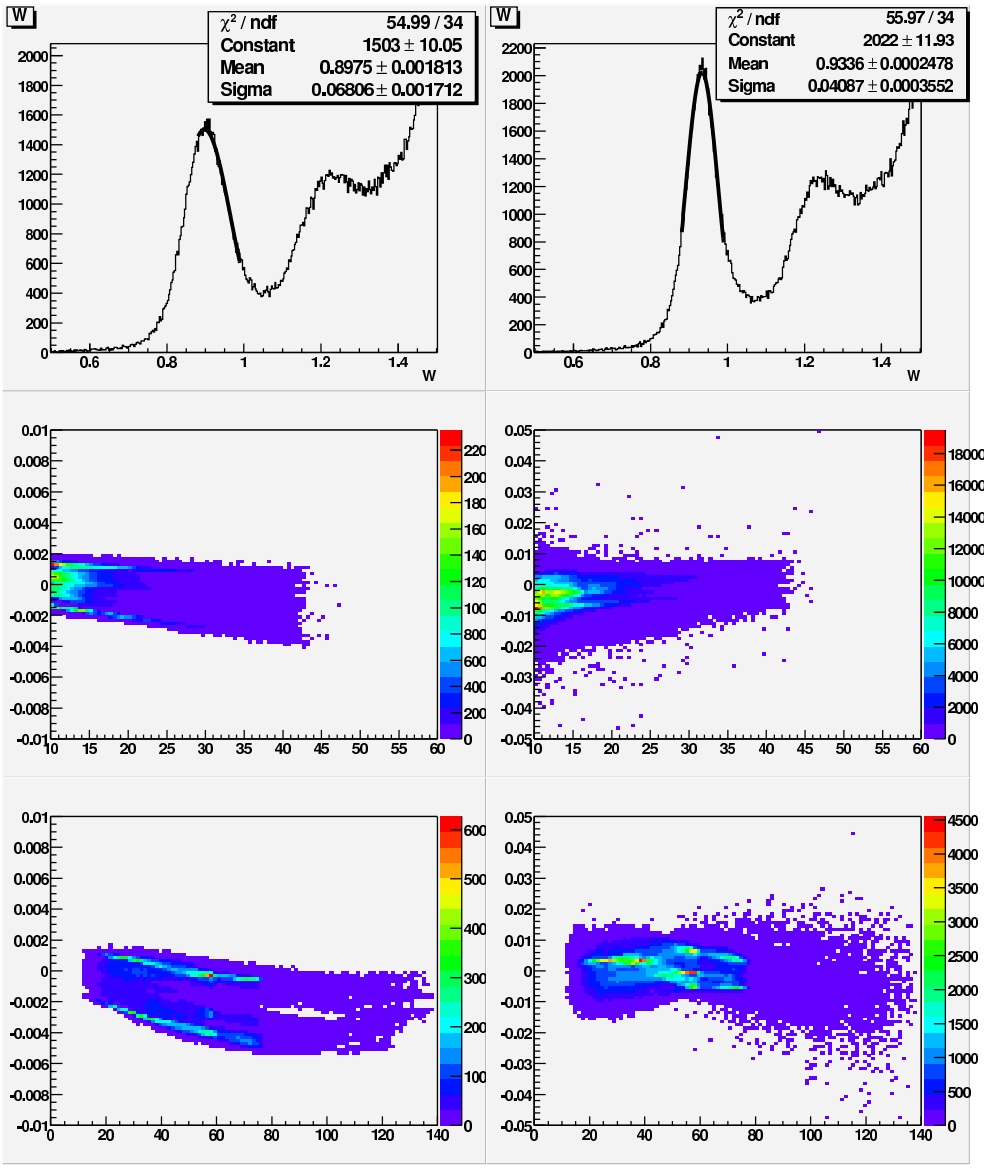

Figure 6: Same as Fig. 5 for outbending torus polarity. Note that the initial W distribution in this case was very broad and far off the nominal centroid of 0.938 GeV, requiring a second iteration of our event selection and fit.

± 2 mrad in angle for electrons and up to 5 mrad for protons. Momentum corrections range up to 2% or more, but are typically smaller than 1%. Figure 7 shows the remaining (slight) ϕ–dependence of the relative energy deviation for inbending elastic events (compare with Fig. 1). Clearly, a further refinement of our method (e.g., adding additional parameters to both parts of the momentum correction) might improve the resolution further, but the gains would likely be marginal.

We also tested our corrections for two reactions that were not included in the fit of our parameters, namely $p(e, e'\pi^+)n$ and $p(e, e'p)X$. The missing mass distribution for the first of these reactions is shown in Fig. 8 both before (top) and after (bottom) momentum and angle corrections. A clear improvement in the width of the neutron peak is seen (the centroid is about 3 MeV too high, probably due to radiative energy loss of the outgoing electron). Similarly, the missing mass distribution for the reaction $p(e, e'p)X$ as shown in Fig. 9 shows visible improvement in the region of small missing masses (around 0 GeV^2) after momentum corrections (red histogram), with less strength in the "unphysical region" $MM^2 < 0$ and a somewhat more apparent separation of neutral pion and photon peaks. The higher mass meson peaks (η and ω) also show slight improvements. Finally, we applied our method to data from EG1b (5.x GeV inbending and outbending runs) using only elastic NH_3(e,e'p) events for the fit. Again, the resolution in W improved dramatically, roughly equivalent with the results from the "standard" momentum correction scheme.

In summary, our momentum correction method results in a clear improvement in momentum and missing mass resolution for different channels and torus settings. While typical results from "ad–hoc" momentum corrections can lead to even narrower distributions, they require a vastly larger number of parameters or a bin-by-bin correction, and they have to be "fine-tuned" for every specific reaction under consideration, without obvious (or reliable) extrapolation into other kinematic regions, reactions or torus settings. The advantage of our method is that it can be uniformly applied to all particles and torus settings, with a very modest number of fit parameters (14 per sector). While one could probably improve the momentum resolution further by adding more fit parameters or trying out different functional forms, we feel that the resolution achieved so far is sufficient for the purpose of E6 analysis. The actual C++ code and the final set of fit parameters are

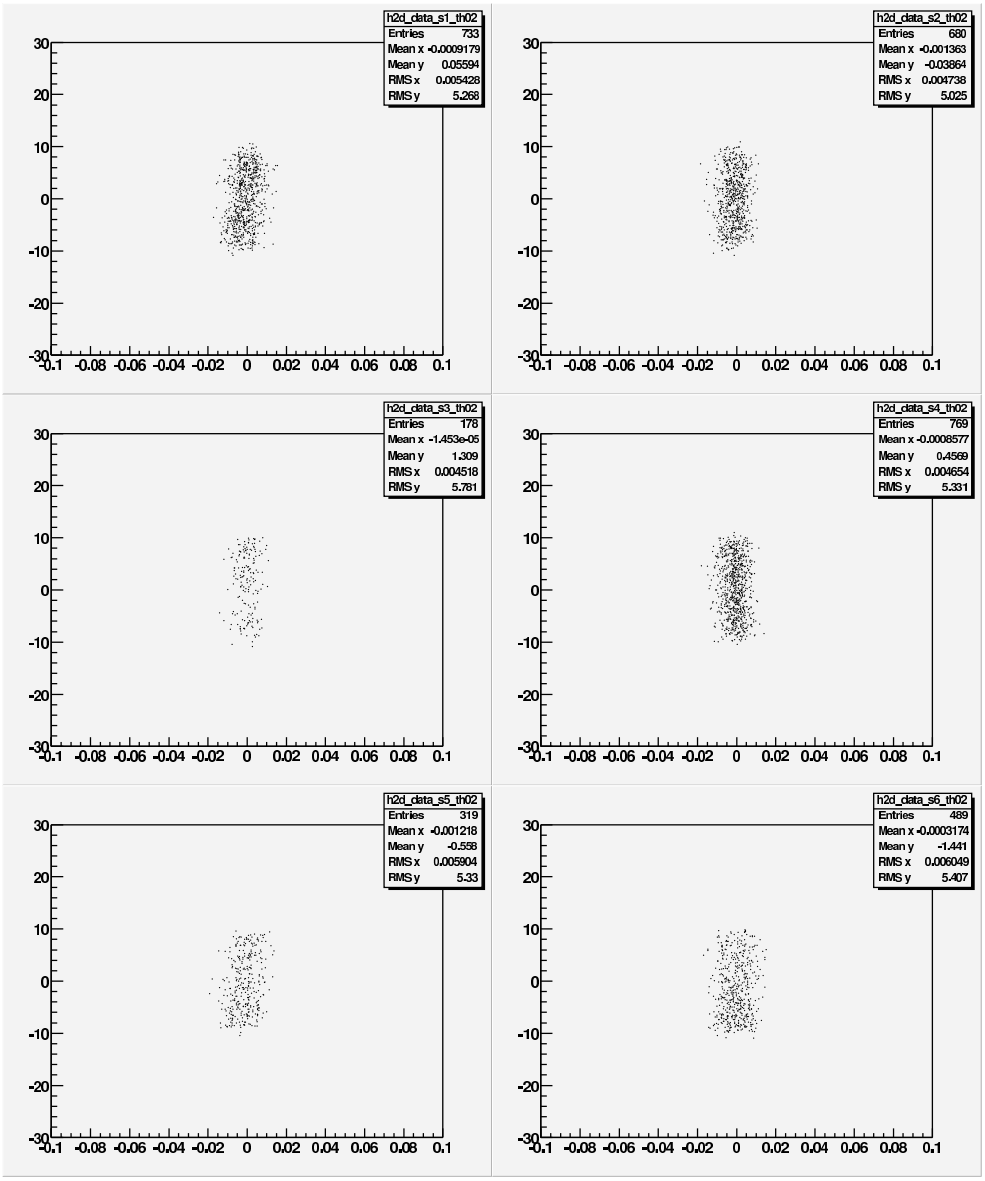

Figure 7: Relative difference between reconstructed electron momentum and calculated momentum for elastic scattering off a proton (see Eq. 1) *after corrections* versus the azimuthal angle ϕ in the sector system (on the y-axis) for all 6 sectors of CLAS. The data are for electron scattering angle $\theta_e = 18^\circ$ and inbending torus polarity.

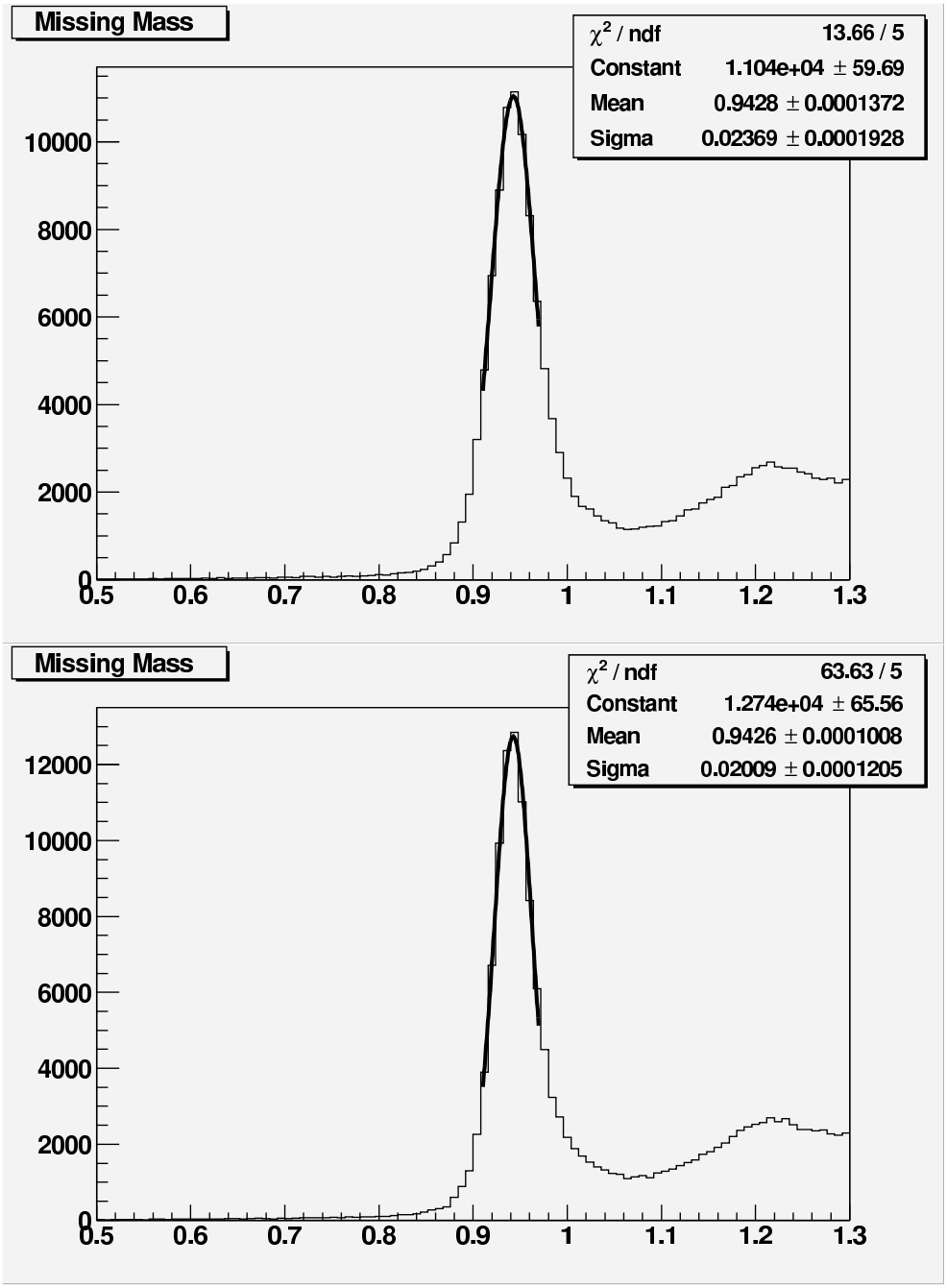

Figure 8: Distribution of missing mass in GeV from the reaction $p(e, e'\pi^+)X$, using data from E6 at 5.75 GeV and inbending torus polarity. The top panel is without momentum corrections and the bottom panel after momentum corrections.

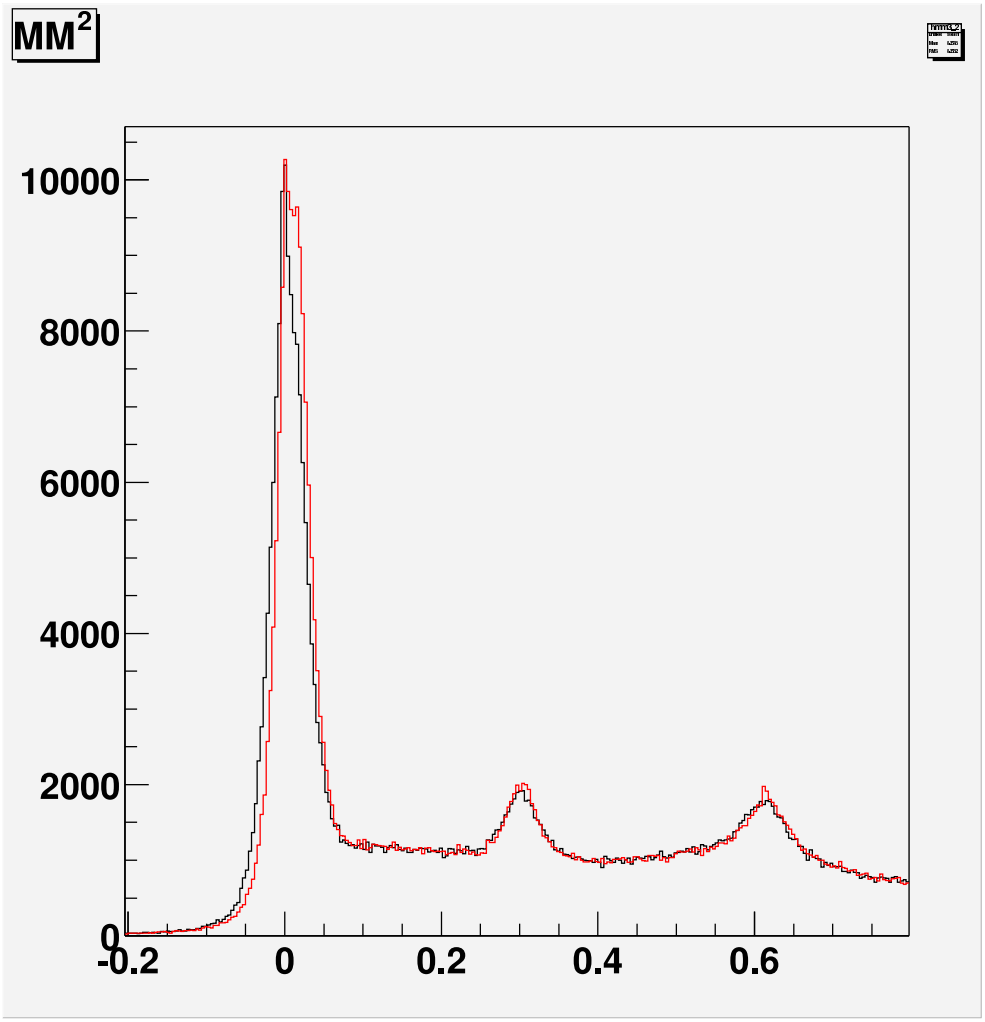

Figure 9: Distribution of squared missing mass in GeV^2 from the reaction $p(e, ep)X$, using data from E6 at 5.75 GeV and inbending torus polarity. We applied a cut of $W > 1.1$ GeV to exclude elastic events. The black line shows the distribution of missing mass before momentum corrections, and the red line afterwards.

listed in the Appendix.

6 Appendix

Below is a listing of the code segment (in C++) used to apply momentum corrections.

```
// Definition of class members

class TE6Ana {
 public:
  // default constructor
  TE6Ana();
  // momentum correction function
  TLorentzVector AngMomCor(TLorentzVector , Double_t , Double_t ,
   Int_t, Double_t);
  public:
  private:
  // momentum correction parametrs
  Double_t par[6][16];
};

// Class constructor

TE6Ana::TE6Ana() {

  // defining input file stream of YAMC parameters

  fstream list;
  list.open("momcor.dat", ios::in);

  // Loading parameters from a file stream above

  for(Int_t mmm=1;mmm<7;mmm++) {
    for(Int_t mmmm=0;mmmm<16;mmmm++) {
      list>>par[mmm-1][mmmm];
    }
  }
}

// Momentum corrections function
```

```
//
// Input:
// V4In - uncorrected 4-vector of the particle
// mass - mass of the particle
// q - charge of the particle (+1. or -1.)
// sector - DC sector
// torus - direction of the torus current (+1. or -1)
//
// Output:
// V4Out - corrected 4-vector of the particle

TLorentzVector TE6Ana::AngMomCor(TLorentzVector V4In, Double_t mass, Double_t q,
 Int_t sector,  Double_t torus) {

  // declaration of used variables
  TLorentzVector V4Out(0.,0.,0.,0);
  Double_t phi=0.,theta=0.,dtheta=0.,factor=0.,dmom=0.,p_cor=0.,term=0.,xi=0.;

  // angle conversion factor
  Float_t rad2deg = 180./TMath::Pi();
  Float_t deg2rad = TMath::Pi()/180.;

  phi=V4In.Phi()*rad2deg;

  // transforming phi: [-30,270] -> [-30,30]

  if(phi<-30.) phi=phi+360.;
  phi=((phi+30.)/60.-(Int_t (phi+30.))/60)*60.-30.;
  phi = phi*deg2rad;

  // ACTUAL CORRECTION STARTS HERE

  factor=V4In.Theta()/(sin(4.*V4In.Theta())*sin(4.*V4In.Theta()));
  if(V4In.Theta()*rad2deg>=22.5) factor=V4In.Theta();

  // Version 5

  flag=sector;

  dtheta=(par[flag-1][0]+par[flag-1][1]*phi)*cos(V4In.Theta())/cos(phi)+
    (par[flag-1][2]+par[flag-1][3]*phi)*sin(V4In.Theta())+par[flag-1][14]*
    cos(V4In.Theta())*cos(V4In.Theta())/cos(phi);;

  // new corrected theta
  theta=V4In.Theta()+dtheta;
```

```
  term=(par[flag-1][4]+par[flag-1][5]*phi)*cos(V4In.Theta())/cos(phi)+
    (par[flag-1][6]+par[flag-1][7]*phi)*sin(V4In.Theta())+par[flag-1][15]*
    cos(V4In.Theta())*cos(V4In.Theta())/cos(phi);

  term=term*V4In.P()*3375./(q*torus*2250.)*factor;

  dmom=term+par[flag-1][8]*cos(theta)+par[flag-1][9]*sin(theta)+
    par[flag-1][10]*sin(2.*theta)+(par[flag-1][11]*cos(theta)+par[flag-1][12]*
   sin(theta)+par[flag-1][13]*sin(2.*theta))*phi;

  // new corrected momentum
  p_cor=V4In.P()*(1.+dmom);
  phi=V4In.Phi();

  V4Out.SetPxPyPzE(p_cor*cos(phi)*sin(theta),p_cor*sin(phi)*sin(theta),
   p_cor*cos(theta),sqrt(p_cor*p_cor+mass*mass));

  return V4Out;
}
```

Below is a listing of all 84 parameters we calculated for E6. There are six groups of parameters $A - O$ for each of the six sectors. The zero entries in between groups are placeholders for possible additional parameters. If interpreted within our model of drift chamber displacements, the first 8 parameters of each sector correspond to displacements of a few mm in both radial direction and along the beam line. In all cases, the displacements of Region III are roughly twice those of Region II, indicating that straight tracks remain straight after taking the displacements into account (the nominal positions of all drift chambers used for cooking the E6 data had been adjusted following a straight track analysis by Steve Morrow et al.). The ϕ–dependent terms indicate rotations of the drift chambers by a few mrad (up to 3 mrad for Region III chambers) – these could be either physical rotations (yaws and rolls) or deviations of the wire hole locations from their nominal values.

```
0.000544
0.002155
-0.000674
-0.000743
-0.002148
0.023805
0.002308
-0.031310
-0.001653
-0.005383
0.003550
-0.017417
-0.000926
0.001714
0
0
0.001530
0.001287
-0.001151
-0.002713
-0.000825
0.014184
0.001793
```

-0.010295
-0.008868
-0.006507
0.007697
-0.010701
-0.002416
0.000805
0
0
0.000877
-0.001526
-0.001301
-0.002379
-0.000797
-0.022676
0.000218
0.015191
-0.008622
-0.005061
0.008700
-0.002587
-0.000883
0.001962
0
0
0.000207
-0.002282
-0.003461
-0.001001
-0.001262
-0.014686
0.001080
0.024763
0.000584
0.002870
0.001482
-0.000476
-0.004804

-0.000161
0
0
-0.000687
0.000899
-0.004286
-0.001755
-0.002735
0.007995
0.001412
-0.009102
-0.003386
0.000869
0.007900
-0.006772
-0.005605
-0.001115
0
0
0.000605
-0.002286
-0.005119
-0.000454
-0.000648
-0.020299
0.000324
0.026492
-0.002688
-0.001121
0.005835
0.004167
-0.003467
-0.001174
0
0